Density Functional Characterization of Methane Metathesis with Cp^*_2MR (M = Sc, Y, Lu; R = Me, $tBuCH_2$). Structural and Kinetic Consequences of Alkyl Steric Bulk

Nathaniel L. Woodrum and Christopher J. Cramer*

Department of Chemistry and Supercomputer Institute, University of Minnesota, 207 Pleasant Street SE, Minneapolis, Minnesota 55455-0431

Received August 19, 2005

The uni- and bimolecular C−H bond metathesis reactions of Cp^*_2ML (Cp^* = pentamethylcyclopentadienide; L = CH_3, $CH_2C(CH_3)_3$; M = Sc, Y, Lu) were modeled with the MPW1K density functional and a relativistic effective-core-potential basis set. This level of theory, when combined with a one-dimensional tunneling model, provides enthalpies of activation that are in good agreement with experiment for known bimolecular reactions of methane with $Cp^*_2ScCH_2C(CH_3)_3$ and $Cp^*_2LuCH_3$. Analysis of theoretical trends as a function of metal and ligand indicates that bimolecular reactions dominate in every case under typical experimental conditions. However, unimolecular reactions proceeding through tuck-in complexes become increasingly competitive with increased steric bulk of the metal alkyl and also with metals having smaller ionic radii. For all of the C−H bond metatheses, quantum-mechanical tunneling is predicted to increase overall reaction rates by 1 to 3 orders of magnitude over the temperature range 284−323 K.

Introduction

The catalytic functionalization of saturated hydrocarbons has been a long-standing goal of organometallic chemistry. Alkyl-, aryl-, and hydridometallocenes of formally d^0 metals have shown potential utility in this regard, as their ability to activate alicyclic and aliphatic C−H bonds has been demonstrated in several instances.[1−5] Recently, Sadow and Tilley[6] reported a catalytic variation on this theme: isobutane is produced when $Cp^*_2ScCH_3$ is reacted with propene in the presence of excess methane, presumably by initial carbometalation and subsequent nondegenerate metathesis with excess methane (Scheme 1). To better understand the nondegenerate metathesis step, Sadow and Tilley[6] studied the kinetics of the reaction of methane with $Cp^*_2ScCH_2C(CH_3)_3$ (i.e., replacing the isobutyl group of the intermediate in the catalytic cycle with a neopentyl). Among other data, they reported an enthalpy of activation (derived from an Eyring plot over the temperature range 284 to 323 K) of 11.4(1) kcal mol^{-1} for a process that followed a bimolecular rate law, a primary kinetic isotope effect of 10.2 for methane compared to d_4-methane at 299 K, and a variety of observations indicating a lack of α-agostic interactions in $Cp^*_2ScCH_2C(CH_3)_3$. Isotopic labeling experiments established that the nondegenerate metathesis reaction does *not* involve the intermediacy of a tuck-in complex (i.e., reaction with one of the Cp* methyl groups in a unimolecular process) at or below the highest experimental temperature. Scheme 2 illustrates the uni- and bimolecular reaction paths.

Scheme 1

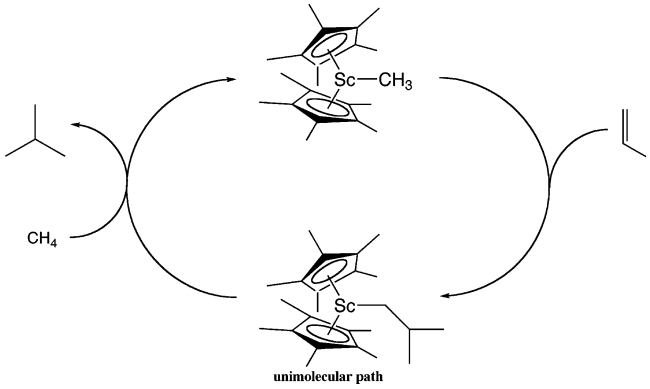

Sherer and one of the present authors[7] previously employed density functional theory (DFT) to theoretically characterize the degenerate methane metathesis reactions of $Cp^*_2MCH_3$ for M = Sc, Y, and Lu. From a chemical perspective, key conclusions of that study included that (i) the activation enthalpies of uni- and bimolecular processes were sensitive to the ionic radii of the metals, with the small size of Sc playing a significant role in modifying its reactivity compared to the experimentally very well studied[8−10] Lu case, and (ii) the contribution of tunneling to metathesis rates remains quite significant even at temperatures as high as 400 K. The latter observation implies that simple interpretation of Eyring plots to derive activation parameters is not strictly valid, since classical transition-state theory does not account for quantum-mechanical tunneling.[11]

* Corresponding author. Phone: (612) 624-0859. Fax: (612) 626-2006. E-mail: cramer@chem.umn.edu.

(1) Wailes, P. C.; Coutts, R. S. P.; Weigold, H. *Organometallic Chemistry of Titanium, Zirconium, and Hafnium*; Academic: New York, 1974.
(2) Watson, P. L.; Parshall, G. W. *Acc. Chem. Res.* **1985**, *18*, 51.
(3) Davies, J. A.; Watson, P. L.; Liebman, J. F.; Greenberg, A. *Selective Hydrocarbon Activation: Principles and Progress*; VCH Publishers: New York, 1990.
(4) Shilov, A. E.; Shul'pin, G. B. *Chem. Rev.* **1997**, *97*, 2879.
(5) Crabtree, R. H. *J. Chem. Soc., Dalton Trans.* **2001**, 2437.
(6) Sadow, A. D.; Tilley, T. D. *J. Am. Chem. Soc.* **2003**, *125*, 7971.
(7) Sherer, E. C.; Cramer, C. J. *Organometallics* **2003**, *22*, 1682.
(8) Watson, P. L. *J. Chem. Soc., Chem. Commun.* **1983**, 276.
(9) Watson, P. L. *J. Am. Chem. Soc.* **1983**, *105*, 6491.
(10) Watson, P. L. In *Selective Hydrocarbon Activation: Principles and Progress*; Davies, J. A., Watson, P. L., Greenberg, A., Liebman, J. F., Eds.; VCH: New York, 1990; p 79.
(11) Steinfeld, J. I.; Francisco, J. S.; Hase, W. L. *Chemical Kinetics and Dynamics*, 2nd ed.; Prentice Hall: New York, 1999.

10.1021/om050720k CCC: $33.50
Publication on Web 11/12/2005

Scheme 2

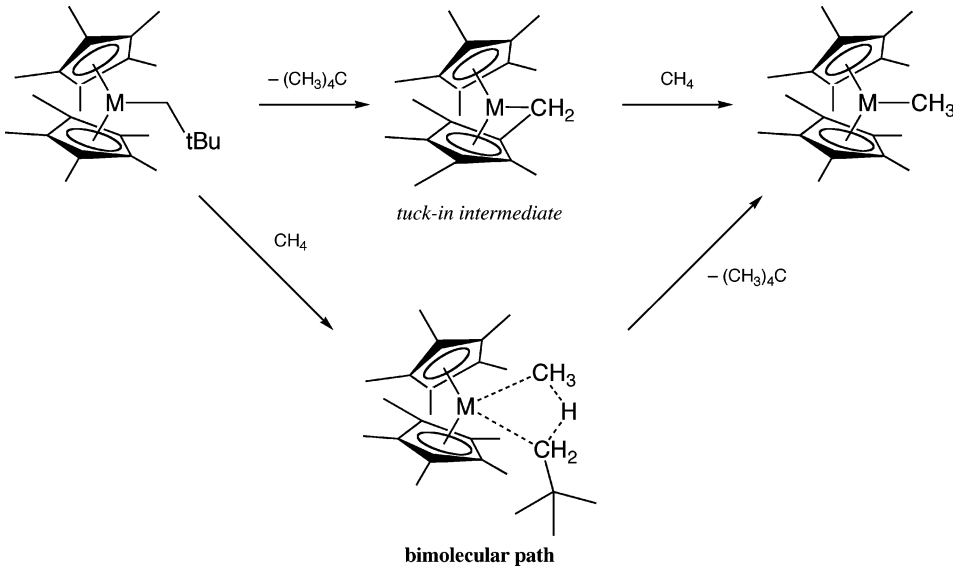

In this work, we extend that prior theoretical analysis to the analogous $Cp^*_2MCH_2C(CH_3)_3$ compounds in order to quantify effects deriving from the introduction of the more sterically demanding neopentyl group in place of methyl. It is clear that the design of successful catalytic systems involving C−H bond metathesis will ultimately require the careful balancing of such steric, as well as electronic, contributions to reactivity.

Methods

All structures were fully optimized at the density functional level of theory[12] using the Gaussian03 suite of electronic structure programs.[13] In this work we employ the hybrid MPW1K functional,[14] which includes 42.8% Hartree−Fock (HF) exchange in Adamo and Barone's modification[15] of the generalized gradient approximation exchange[16] and correlation[17] functionals of Perdew and Wang. The amount of HF exchange in the MPW1K functional was optimized against a training set of hydrogen-atom transfer activation energies, and thus this functional represents a particularly good choice for the study of C−H bond metathesis reactions. MPW1K has also been demonstrated to do well in predicting a wide variety of other structural and thermochemical data.[18] For all metal atoms we used the relativistic effective core potential basis of Stoll et al.,[19] while the 6-31G(d,p) basis set[20] was used for H and C. All restricted Kohn−Sham determinants were verified to be stable to spin-symmetry breaking.

Analytic frequency calculations were carried out in order to verify the nature of all stationary points as either minima or transition-state (TS) structures. The frequencies, scaled by a factor of 0.9515,[21] were also employed to compute molecular partition functions and thermal contributions to the enthalpy using the standard rigid-rotor-harmonic-oscillator approximation.[18] Because structures incorporating Cp* typically had many very small vibrational frequencies (below 20 cm^{-1}), we avoid discussion of molecular free energies, since absolute entropies predicted by the rigid-rotor-harmonic-oscillator approximation tend to be unreliable in such instances.

The reaction coordinates for the various C−H bond metatheses examined herein show substantial hydrogenic motion in their associated TS structures, so that it is reasonable to expect the reaction rate to include a substantial contribution from light-atom tunneling even at reaction temperatures on the order of 350 K. In such cases, the observed rate constant k_{obs} may be written[11,18]

$$k_{obs} = \kappa(T)k_{class} \tag{1}$$

where κ is the temperature-dependent quantum-mechanical transmission coefficient and k_{class} is the rate constant that would be observed in the absence of quantum effects. In addition to tunneling, nonclassical reflection is included in κ, but the latter tends to have much less effect than tunneling on observed rates until temperatures become very high.

Sadow and Tilley[6] reported experimental activation enthalpies and entropies for the reaction of methane with $Cp^*_2ScCH_2C(CH_3)_3$ derived from the transition-state theory relationship[11,18]

$$\ln\left(\frac{k_{obs}}{T}\right) = \left(-\frac{\Delta H^{\ddagger}}{R}\right)\left(\frac{1}{T}\right) + \left(\frac{\Delta S^{\ddagger}}{R}\right) + \ln\left(\frac{k_B}{h}\right) \tag{2}$$

where T is temperature, R is the universal gas constant, k_B is Boltzmann's constant, and h is Planck's constant. Thus, a plot of $\ln(k_{obs}/T)$ vs $1/T$ provides a best-fit line having slope $-\Delta H^{\ddagger}/R$ and the intercept permits determination of $\Delta S^{\ddagger}$.

(12) Koch, W.; Holthausen, M. C. *A Chemist's Guide to Density Functional Theory*; Wiley-VCH: Weinheim, 2000.

(13) Frisch, M. J.; Trucks, G. W.; Schlegel, H. B.; Scuseria, G. E.; Robb, M. A.; Cheeseman, J. R.; Montgomery, J. A.; Vreven, T.; Kudin, K. N.; Burant, J. C.; Millam, J. M.; Iyengar, S. S.; Tomasi, J.; Barone, V.; Mennucci, B.; Cossi, M.; Scalmani, G.; Rega, N.; Petersson, G. A.; Nakatsuji, H.; Hada, M.; Ehara, M.; Toyota, K.; Fukuda, R.; Hasegawa, J.; Ishida, M.; Nakajima, T.; Honda, Y.; Kitao, O.; Nakai, H.; Klene, M.; Li, X.; Knox, J. E.; Hratchian, H. P.; Cross, J. B.; Adamo, C.; Jaramillo, J.; Gomperts, R.; Stratmann, R. E.; Yazyev, O.; Austin, A. J.; Cammi, R.; Pomelli, C.; Ochterski, J. W.; Ayala, P. Y.; Morokuma, K.; Voth, G. A.; Salvador, P.; Dannenberg, J. J.; Zakrzewski, V. G.; Dapprich, S.; Daniels, A. D.; Strain, M. C.; Farkas, O.; Malick, D. K.; Rabuck, A. D.; Raghavachari, K.; Foresman, J. B.; Ortiz, J. V.; Cui, Q.; Baboul, A. G.; Clifford, S.; Cioslowski, J.; Stefanov, B. B.; Liu, G.; Liashenko, A.; Piskorz, P.; Komaromi, I.; Martin, R. L.; Fox, D. J.; Keith, T.; Al-Laham, M. A.; Peng, C. Y.; Nanayakkara, A.; Challacombe, M.; Gill, P. M. W.; Johnson, B.; Chen, W.; Wong, M. W.; Gonzalez, C.; Pople, J. A. *Gaussian 03*, revision B.05; Gaussian, Inc.: Pittsburgh, PA, 2003.

(14) Lynch, B. J.; Fast, P. L.; Harris, M.; Truhlar, D. G. *J. Phys. Chem. A* **2000**, *104*, 4811.

(15) Adamo, C.; Barone, V. *J. Chem. Phys.* **1998**, *108*, 664.

(16) Perdew, J. P.; Wang, Y. *Phys. Rev. B* **1986**, *33*, 8800.

(17) Perdew, J. P. In *Electronic Structure of Solids '91*; Ziesche, P., Eschrig, H., Eds.; Akademie Verlag: Berlin, 1991; p 11.

(18) Cramer, C. J. *Essentials of Computational Chemistry*, 2nd ed.; John Wiley & Sons: Chichester, 2004.

(19) Stoll, H.; Metz, B.; Dolg, M. *J. Comput. Chem.* **2002**, *23*, 767.

(20) Hehre, W. J.; Radom, L.; Schleyer, P. v. R.; Pople, J. A. *Ab Initio Molecular Orbital Theory*; Wiley: New York, 1986.

(21) Lynch, B. J.; Truhlar, D. G. *J. Phys. Chem. A* **2001**, *105*, 2936.

Note, however, that the use of eq 2 to determine thermodynamic activation parameters is appropriate only with *classical* rate constants. When observed rate constants from reactions whose rates include substantial contributions from tunneling are used in eq 2, derived activation enthalpies and entropies tend to values considerably less positive and more negative, respectively, than those determined from the statistical mechanical partition functions of the relevant reactants and transition-state structures. In such instances, the comparison of "experimental" and computed thermodynamic activation parameters is not particularly meaningful, since the latter are indeed computed directly from the molecular partition functions.

One can, however, compute classical rate constants k_{class} at a given temperature as k_{obs} divided by $\kappa(T)$ (cf. eq 1). A subsequent plot of $\ln(k_{class}/T)$ vs $1/T$ then provides a best-fit line having slope $-\Delta H^{\ddagger}/R$ where the new, classical $\Delta H^{\ddagger}$ may be compared directly to the value derived from computation. Sherer and one of us have previously demonstrated that this approach resolves an otherwise large difference of about 8 kcal mol^{-1} between the Eyring-plot-derived and theoretical enthalpy of activation for methane metathesis involving $Cp^*_2LuCH_3$.[7]

To estimate κ, we employ the truncated parabola method of Skodje and Truhlar.[18,22] In this approximation, the transmission coefficient associated with quantum effects on the reaction coordinate, κ, is computed as

$$\kappa(T) = \begin{cases} \dfrac{\beta}{\beta-\alpha}\{e^{[(\beta-\alpha)(\Delta V^{\ddagger}-V)]}-1\} & \alpha \le \beta \\ \dfrac{\beta\pi/\alpha}{\sin(\beta\pi/\alpha)} - \dfrac{\beta}{\alpha-\beta}e^{[(\beta-\alpha)(\Delta V^{\ddagger}-V)]} & \alpha \ge \beta \end{cases} \quad (3)$$

where

$$\alpha = \frac{2\pi}{h\mathrm{Im}(\nu^{\ddagger})} \quad (4)$$

$$\beta = \frac{1}{k_B T} \quad (5)$$

$\Delta V^{\ddagger}$ is the zero-point-including activation barrier, V is the zero-point-including potential-energy difference between reactants and products (zero in the case of the symmetric metathesis reaction, nonzero otherwise), and $\mathrm{Im}(\nu^{\ddagger})$ is the (scaled) magnitude of the imaginary vibration.

With respect to the experimental rate constants, Sadow and Tilley[6] measured k_{obs} values at 284.15, 299.15, 313.15, and 323.15 K. They report specific values of 4.1×10^{-4} and 2.0×10^{-3} M^{-1} s^{-1} at 299.15 and 232.15 K, respectively. We infer values of 1.29×10^{-4} and 6.72×10^{-4} M^{-1} s^{-1} for the remaining two rate constants at 284.15 and 313.15 K, respectively; these values best reproduce the reported enthalpy and entropy of activation derived from the Eyring plot over all 4 points ($\Delta H^{\ddagger}$ (kcal mol^{-1}) of 11.41 vs reported 11.4(1) and $\Delta S^{\ddagger}$ (eu) of -36.2 vs reported $-36(1)$).

Results and Discussion

Nomenclature. We will refer to $Cp^*_2MCH_3$ and $Cp^*_2MCH_2C(CH_3)_3$ equilibrium structures as **1** and **2**, respectively. Their uni- and bimolecular metathesis transition-state (TS) structures will be indicated by the suffixes **uni**‡ and **bi**‡, respectively. The unimolecular reaction of either **1** or **2** leads to a tuck-in complex which will be referred to as **3**. Note that, by microscopic reversibility, the subsequent reaction of **3** with methane passes through TS structure **1uni**‡ to produce **1** irrespective of whether **3** was derived from **1** or **2** initially. When only a cardinal is specified for a structure, the reference is generic. If a particular metal is implied, the cardinal will be modified with a suffix, e.g., **2**-Sc refers to $Cp^*_2ScCH_2C(CH_3)_3$.

Metallocene Structure. Selected geometrical parameters for **1**−**3**, respectively, are collected in Tables 1−3 (see Scheme 2 for reactions). The optimized structures for **2**-Sc, **2uni**‡-Sc, **2bi**‡-Sc, and **3**-Sc are shown in Figure 1 as ball-and-stick models. The gross structural details are not sufficiently different with other metals to warrant additional figures; full geometries for all species are available as Supporting Information.

All structures **1** and **2** exhibit expected trends: Ligand−metal bond lengths are shorter for Sc than for Y, as expected for a

Table 1. Selected Bond Distances (Å) and Bond Angles (deg) in 1 and 2 at the MPW1K Level[a]

compound	M	*r*MC	*r*MΩ[b]	∠ΩMΩ
1	Sc[c]	2.233	2.176	143.8
		(2.243)	(2.171)	(144.6)
	Y	2.396	2.363	142.8
	Lu	2.340	2.291	143.2
2	Sc[d]	2.283	2.208	138.4
		(2.286)	(2.213)	(138.8)
	Y	2.434	2.389	138.0
	Lu	2.385	2.314	138.0

[a] In columns, C refers to the metal-bound carbon and Ω refers to the centroid of a Cp* ring. [b] Average of two distances. [c] Values in parentheses are from a single-crystal X-ray structure; see ref 23. [d] Values in parentheses are from a single-crystal X-ray structure; see ref 6.

Table 2. Selected Bond Distances (Å) and Bond Angles (deg) in 1uni‡, 2uni‡, 1bi‡, and 2bi‡ at the MPW1K Level[a]

compound	M[b]	*r*MC[c]	*r*MΩ	*r*MH	*r*CH[c]	∠CMC	∠ΩMΩ
1uni‡	Sc	2.359	2.146	1.912	1.444	73.3	144.7
	1369.5*i*	2.431			1.467		
	Y	2.525	2.326	2.081	1.448	69.0	145.0
	1419.4*i*	2.593			1.485		
	Lu	2.450	2.251	2.015	1.444	70.9	145.3
	1396.5*i*	2.535			1.490		
2uni‡	Sc	2.433	2.170	1.959	1.533	72.9	138.5
	1384.4*i*	2.457			1.411		
	Y	2.541	2.341	2.115	1.526	69.6	140.0
	1455.3*i*	2.612			1.444		
	Lu	2.484	2.270	2.053	1.519	71.1	139.5
	1440.9*i*	2.558			1.446		
1bi‡	Sc	2.380	2.205	1.881	1.417	73.1	141.5
	1292.0*i*						
	Y	2.532	2.373	2.045	1.431	68.8	141.7
	1325.3*i*						
	Lu	2.465	2.308	1.983	1.433	71.1	141.9
	1319.2*i*						
2bi‡	Sc	2.430	2.230	1.910	1.522	73.8	137.2
	1277.4*i*	2.386			1.372		
	Y	2.525	2.393	2.064	1.522	70.3	137.8
	1343.9*i*	2.543			1.396		
	Lu	2.482	2.325	2.002	1.519	72.1	137.6
	1335.0*i*	2.472			1.397		

[a] In columns, C refers to the incoming and outgoing metal-bound carbon atoms, Ω refers to the centroid of a Cp* ring, and H refers to the hydrogen atom in flight between the two alkyl groups in the metathesis. [b] The scaled imaginary frequency associated with the TS structure is also listed. [c] The first number refers to the C atom to which H is being transferred and the second to the C atom from which it is being taken. These two values are equal by symmetry for **1bi**‡.

Table 3. Selected Bond Distances (Å) and Bond Angles (deg) in 3 at the MPW1K Level[a]

M	*r*MC	*r*MΩ[b]	∠ΩMΩ
Sc	2.322	2.090	155.2
Y	2.498	2.289	151.7
Lu	2.434	2.210	153.6

[a] In columns, C refers to the metal-bound carbon and Ω refers to the centroid of a Cp* ring. [b] Average of two distances.

(22) Skodje, R. T.; Truhlar, D. G. *J. Phys. Chem.* **1981**, *85*, 624.

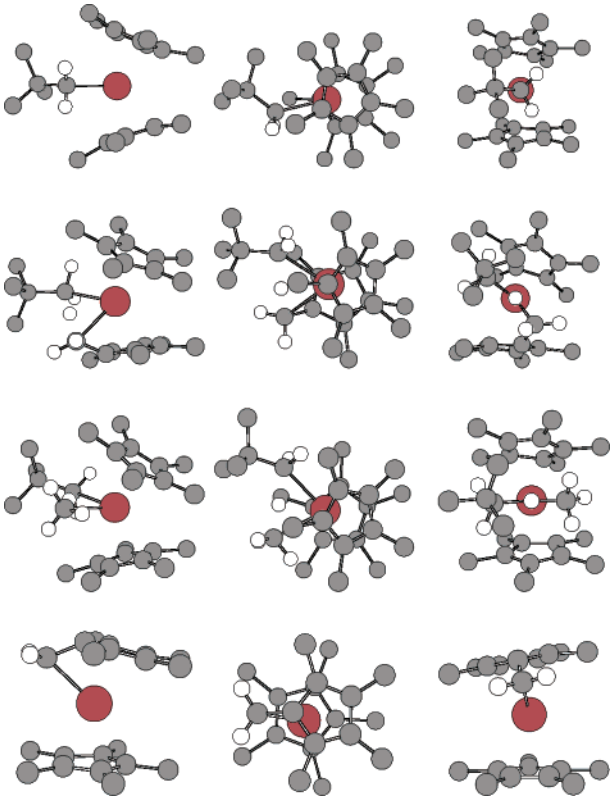

Figure 1. Side (left), top (center), and front (right) views of, from top to bottom, structures for **2**-Sc, **2uni**‡-Sc, **2bi**‡-Sc, and **3**-Sc optimized at the MPW1K level. For clarity, all hydrogen atoms have been removed except those attached to or being transferred between carbon atoms bonded to Sc.

third-row/fourth-row progression; ligand−metal bond lengths for Lu are slightly shorter than for Y, also as expected from a combination of the lanthanide contraction and relativistic effects. The steric influence of the neopentyl group compared to a methyl makes itself felt in a roughly 5 deg smaller bite angle between the two Cp* rings and a metal−carbon bond length that is about 0.05 Å longer.

Comparisons between the computed structures for **1**-Sc and **2**-Sc and available X-ray crystal structures for these species[6,23] demonstrate the excellent performance of the MPW1K method for these geometries. Consistent with the analysis of Sadow and Tilley noted above, there is no evidence of α-agostic interactions in the MPW1K structure for **2**-Sc.

In the TS structures, the primary difference between stationary points derived from **1** and **2** is that both kinds of transition states, **uni**‡ and **bi**‡, are earlier in the neopentyl cases compared to the methyl cases. This is most easily seen in the C−H distances, where the breaking C−H bonds are shorter for structures derived from **2** compared to analogous structures derived from **1** and the forming bonds are correspondingly longer. The same trend is true for changes in metal−carbon bond lengths compared to reactants (one must focus on changes rather than absolute bond lengths because of the 0.05 Å difference in the reactant lengths noted above). The carbon atoms for departing methane fragments have progressed further toward dissociation than have the metal-bound carbon atoms for departing neopentanes in analogous TS structures. The earlier transition states in the reaction paths for **2** reflect the greater exothermicity associated with ejection of the bulky neopentyl group compared to a methyl group.

(23) Thompson, M. E.; Baxter, S. M.; Bulls, A. R.; Burger, B. J.; Nolan, M. C.; Santasiero, B. D.; Schaefer, W. P.; Bercaw, J. E. *J. Am. Chem. Soc.* **1987**, *109*, 203.

Table 4. 299 K Relative Enthalpies (kcal mol^{-1}) for Stationary Points on the Reaction Paths of 1 and 2 and Quantum-Mechanical Transmission Coefficients (unitless) for Their Rate-Determining Steps

Unimolecular Reactions

	relative enthalpies					
metal	**1**	**1uni**‡	**3**	**1uni**‡	**1**	κ_{299}
Sc	0.0	30.6	8.0	30.6	0.0	110
Y	0.0	32.3	13.3	32.3	0.0	190
Lu	0.0	32.8	14.1	32.8	0.0	120

	relative enthalpies					
metal	**2**	**2uni**‡	**3**	**1uni**‡	**1**	κ_{299}
Sc	0.0	27.2	−7.8	14.8	−15.8	280
Y	0.0	29.4	2.7	21.7	−10.6	1200
Lu	0.0	29.8	1.8	20.5	−12.2	1000

Bimolecular Reactions

	relative enthalpies			
metal	**1**	**1bi**‡	**1**	κ_{299}
Sc	0.0	23.2	0.0	32
Y	0.0	19.6	0.0	45
Lu	0.0	20.9	0.0	44

	relative enthalpies			
metal	**2**	**2bi**‡	**1**	κ_{299}
Sc	0.0	19.7	−15.8	24
Y	0.0	17.0	−10.6	48
Lu	0.0	18.1	−12.2	47

With respect to comparing **uni**‡ and **bi**‡ structures, the former appear to be somewhat more strained than the latter in every instance, as judged by longer distances between the H atoms in flight and the C atoms between which they are being transferred for analogous uni- and bimolecular TS structures. The H atoms in flight are also further from the metal in the unimolecular TS structures compared to their bimolecular counterparts. Computed imaginary frequencies are consistent with this assignment of greater strain as well, being larger in magnitude for all **uni**‡ structures compared to their **bi**‡ analogues.

The tuck-in complexes **3** are not especially remarkable. Their most noteworthy features are ligand bite angles in excess of 150° and a metal−carbon bond length that is always about 0.1 Å longer than that in the corresponding structure of **1**. This latter feature presumably introduces considerable strain energy into the system (vide infra).

Unimolecular Alkane Displacement. Table 4 provides 299 K enthalpies for all stationary points on all alkane metathesis reaction pathways (the enthalpies are stoichiometrically balanced; thus, for instance, relative enthalpies for **3** always include a contribution from isolated methane or neopentane). Quantum-mechanical transmission coefficients are also provided. Note that the reaction of a tuck-in complex **3** with methane always proceeds through **1uni**‡ to generate **1** irrespective of whether that tuck-in complex originated from **1** or **2** (although obviously if it originated from **1**, the net reaction is thermoneutral, being solipsistic).

For all three metals, the activation enthalpies for **2** are about 3 kcal mol^{-1} lower than for **1**, reflecting the steric strain from the neopentyl group released in the TS structure. In the case of Sc, the tuck-in structure **3**-Sc is substantially lower in enthalpy than the reactant **2**-Sc. For the other two metals, the larger ionic radii destabilize the tuck-in complexes sufficiently that the

unimolecular reactions generating **3** from **2** are endothermic, but only by a small margin, and much less so than is computed for **1**.

Interestingly, the 299 K transmission coefficients for the unimolecular reactions of **1** are relatively large, on the order of 100, and those for **2** are larger still, reaching in excess of 1000. These significant values reflect the high degree of hydrogenic motion in the reaction coordinate (which gives rise to an imaginary frequency that is relatively large in magnitude) as well as a large potential-energy barrier to reaction. The larger magnitude of the κ values for **2** compared to **1** derives from two factors. First, the greater endothermicity associated with the reactions of **1** prevent tunneling from energy levels below the ground state of **3**. Second, the larger imaginary frequencies associated with **2** compared to **1** imply narrower barriers. The former effect contributes about twice as much to the computed differences as the latter.

Bimolecular Alkane Metathesis. The data in Table 4 show that the activation enthalpy of **2** for reaction with methane is always lower than the corresponding value for **1**, which is not surprising given relief from the greater steric bulk of the neopentyl ligand compared to the methyl in the TS structure. The difference is 3.5, 2.6, and 2.8 kcal mol^{-1} for Sc, Y, and Lu, respectively, tracking inversely with the ionic radii of the metals, which affects the steric sensitivity of the reaction. The trend in differential activation enthalpies is also directly proportional to the exothermicities of the overall reactions for **2**, consistent with the Curtin−Hammett principle.[24]

At 299 K, the transmission coefficients for all six bimolecular metatheses are between 20 and 50. This relative insensitivity reflects the rather small variation in imaginary frequencies for the various reactions as well as the modest height of the barriers.

To probe further the quantitative utility of the calculations, we note that Watson and Parshall[2] measured 343 K rate constants for the bimolecular reactions of all three cases of **1** with methane. The ratio of rate constants that they reported was 5.7:1:0.022 for Y:Lu:Sc. We may use transition-state theory (rearranging eq 2 and making the mild assumptions of identical entropies of activation and transmission coefficients) to determine that this implies activation enthalpy differences of 1.2 kcal mol^{-1} between Y and Lu, 3.8 kcal mol^{-1} between Y and Sc, and 2.6 kcal mol^{-1} between Lu and Sc. The theoretical predictions in Table 4 for these comparisons at 299 K (the temperature dependences of the activation enthalpies are very, very small) are 1.3, 3.6, and 2.3 kcal mol^{-1}, respectively, which is an average error of only 0.2 kcal mol^{-1}. Such outstanding agreement is further validation of the MPW1K method for hydrogen-atom transfer reactions.

Table 4 further indicates that for all metals and either choice of alkyl ligand the bimolecular process is favored over the unimolecular one, with the difference being largest for Y and Lu and somewhat smaller for Sc. Of course, any analysis of rates for a unimolecular process compared to a bimolecular one must take into account the concentration of the reacting partners in the bimolecular process. Clearly at sufficiently low methane concentrations one would eventually find the unimolecular processes to be kinetically dominant, although in such instances it would also be the case that the tuck-in complexes would be free energy sinks rather than simply intermediates in net metatheses. Indeed, in the case of **1**-Sc Thompson et al.[23] observed that prolonged heating of the molecule at 353 K led to methane production and a yellow, crystalline solid that, although not possible to characterize completely, had a ^{1}H NMR spectrum consistent with it being **3**-Sc.

Table 5. Transmission Coefficients Predicted for Reaction through 2bi‡-Sc and Observed and Classical Rate Constants at Different Temperatures[a]

T, K	$k_{obs} \times 10^5$, s^{-1}	κ	$k_{class} \times 10^5$, s^{-1}
284	12.9	64.9	0.199
299	41.0	23.9	1.71
313	67.2	12.8	5.25
323	200.	9.28	21.6

[a] See eqs 1−5 and Computational Methods.

Note that although we do not consider our computed entropies of activation to be quantitatively accurate owing to the presence of many, many low-frequency normal modes, and thus refrain from discussing them, nevertheless the entropy of activation for the bimolecular process will clearly be much more negative than that for the unimolecular one. As such, modification of the reaction temperature could also be used to tune between the two pathways, particularly in the case of Sc, where the difference in activation enthalpies is the smallest.

A final feature discriminating the bimolecular processes from their unimolecular counterparts is that the computed 299 K transmission coefficients are nearly 2 orders of magnitude larger for the latter compared to the former. At that temperature, however, a 100-fold increase in rate is equivalent to an activation-enthalpy lowering of only 2.7 kcal mol^{-1}.[18] As the differences in activation enthalpies between the uni- and bimolecular processes are significantly larger than this value, differential tunneling is not sufficient to reverse the reactivity preference, at least not at experimental temperatures and methane concentrations.

Tunneling Effects on Eyring Analysis for 2-Sc. From an Eyring plot, Sadow and Tilley[6] determined the enthalpy and entropy of activation for methane exchange through **2bi**‡-Sc to be 11.4 kcal mol^{-1} and −36 eu, respectively. While we have emphasized above the excellent performance of theory with respect to predicting the *relative* activation enthalpies for Sc vs Y vs Lu, the "experimental" value for **2**-Sc is in very poor agreement with the computed value of 19.7 kcal mol^{-1}. However, as noted in the Computational Methods section, the problem lies in the use of an Eyring plot to determine activation parameters when quantum-mechanical tunneling plays a variable role over the experimental temperature range. In particular, since tunneling becomes increasingly important at lower temperatures, Eyring plots over temperature ranges where tunneling makes significant contributions to the rate tend to predict, as artifacts, enthalpies of activation that are lower than those associated with the zero-point-including potential-energy surface.

If tunneling contributions are removed from k_{obs} using eq 1, the remaining k_{class} values may themselves be employed in an Eyring plot. Using the data in the right-hand column of Table 5 for such a plot ($R^2 = 0.989$) results in a "corrected experimental" *semiclassical* enthalpy of activation of 20.5 kcal mol^{-1} and entropy of activation of −12.3 eu. Thus, accounting for quantum-mechanical tunneling corrects the apparent activation enthalpy by 9.1 kcal mol^{-1}. Moreover, the corrected value is in excellent agreement with the theoretically predicted value of 19.7 kcal mol^{-1} in Table 4.

Kinetic Isotope Effects. Sadow and Tilley[6] also measured kinetic isotope effects for the reaction of **2**-Sc with CD_4 and CH_2D_2. At 299 K they found $k_H/k_D = 10.2$ for reaction of **2**-Sc with CH_4 vs CD_4. At the MPW1K level, we predict the change in zero-point-vibrational energy (ZPVE) on going from reactants to the TS structure to be 0.4 kcal mol^{-1} greater for reaction

(24) Curtin, D. Y. *Rec. Chem. Prog.* **1954**, *15*, 111.

with CD_4 compared to CH_4, which difference would lead to a KIE of 2.0. In addition, we predict 299 K κ values for reaction with CH_4 and CD_4 of 23.9 and 2.86, respectively. Differential tunneling is thus predicted to increase the primary KIE to 16.4, a value that is somewhat larger than the measured value of 10.2. The difference between theory and experiment may simply reflect the difficulty in accurately computing the quantum-mechanical transmission coefficient κ as it becomes large, as it does for H. In addition, the harmonic approximation[18] used in the computation of the vibrational frequencies and ZPVEs may not be entirely adequate for the extremely sterically congested TS structure for H-atom transfer. Potentials steeper than harmonic would favor D substitution over H (because of the increased difference in ZPVE between the two) and move the predicted KIE into better agreement with experiment. However, the very high dimensionality of the potential energy surface for this reaction does not make further exploration of this detail practical.

With respect to reaction of **2**-Sc with CH_2D_2, in this case Sadow and Tilley[6] reported the "internal" primary kinetic isotope effect by measurement of the ratio of products d_2-**1**-Sc, deriving from H-atom transfer to neopentane, vs d_1-**1**-Sc, deriving from D-atom transfer to neopentane. Their reported value of 5.2, however, is somewhat puzzling at first glance given the measured KIE for CH_4 vs CD_4. Abstraction of a H or D atom from CH_2D_2 should be accelerated relative to CH_4 or decelerated relative to CD_4, respectively, by a normal secondary KIE.[25] Thus, one might expect the *primary* KIE for CH_2D_2 to be *increased* relative to that for CH_4 vs CD_4. Indeed, after accounting for differential tunneling we predict a primary KIE of 18.2 at the MPW1K level.

This issue is subject to additional analysis because Sadow and Tilley[6] reported that the reaction of **2**-Sc with CH_2D_2 is 1.78 times slower than the equivalent reaction with CH_4. If we assign the relative reaction rate of an individual H-atom abstraction in CH_4 to be 1.00 and arbitrarily assume the secondary KIE to increase that rate in CH_2D_2 to 1.05, the relative rate for an individual D-atom abstraction must be 0.074 to result in a 1.78-fold decrease (i.e., rate for CH_4 is statistical $4 \times 1.00 = 4.00$ and rate for CH_2D_2 is statistical $2 \times 1.05 +$ statistical $2 \times 0.074 = 2.25$; ratio of 4:2.25 is 1.78). The ratio of 1.05 to 0.074 corresponds to a primary KIE of 14.2.

If one applies this simple algebraic analysis in reverse, accepting the primary KIE to be 5.2, the predicted rate of an individual H-atom abstraction becomes 0.897, while that for a D-atom abstraction becomes 0.173. This leads to the puzzling conclusion that the rate of H-atom abstraction is suppressed by roughly 10% by replacing 2 H atoms of CH_4 with D, while the rate of D-atom abstraction is accelerated by 175% or more by replacing 2 D atoms of CD_4 with H (the magnitude of the acceleration depends on whether one uses the experimental or computed primary KIE for CH_4 vs CD_4).

One possible solution to this apparent paradox is that product analysis was complicated by continued metathesis of the initially formed d_2-**1**-Sc and d_1-**1**-Sc isotopomers with excess CH_2D_2. We predict an *equilibrium* isotope effect very close to 1.0, so any degree of continuing metathesis would be expected to reduce the apparent KIE. However, the description of the original experimental protocol[6] does not permit us to assess this hypothesis further.

Acknowledgment. This work was supported by NSF CHE-0203446.

Supporting Information Available: Cartesian coordinates for all optimized theoretical structures. This material is available free of charge via the Internet at http://pubs.acs.org.

OM050720K

(25) Carpenter, B. K. *Determination of Organic Reaction Mechanisms*; Wiley-Interscience: New York, 1984.